IL NUOVO CIMENTO **42 C** (2019) 105
DOI 10.1393/ncc/i2019-19105-y

Colloquia: EuNPC 2018

Dynamics of nucleus-nucleus collisions and neutron rearrangement in time-dependent approach

V. V. Samarin([1])([2]), Yu. E. Penionzhkevich([1])([3]), M. A. Naumenko([1]), N. K. Skobelev([1]) and Yu. G. Sobolev([2])

([1]) *Joint Institute for Nuclear Research - Dubna, Russia*
([2]) *Dubna State University - Dubna, Russia*
([3]) *National Research Nuclear University - Moscow, Russia*

received 5 February 2019

Summary. — The dynamical approach based on numeric solution of the time-dependent Schrödinger equation is applied to description of transfer and rearrangement of nucleons in nucleus-nucleus collisions. The results of calculation of neutron transfer cross sections for reaction ^{6}He + ^{197}Au and total reaction cross sections for reactions ^{6}He + ^{28}Si, ^{9}Li + ^{28}Si are in agreement with experimental data.

1. – Theory

The processes of neutron transfer are widely studied both experimentally and theoretically. For theoretical description of neutron rearrangement and transfer in collisions of atomic nuclei we used the time-dependent Schrödinger equation (TDSE) approach [1, 2] for the external neutrons combined with the classical equations of motion of atomic nuclei with centers $\vec{r}_1(t), \vec{r}_2(t)$. The evolution of the components ψ_1, ψ_2 of the spinor wave function $\Psi(\vec{r}, t)$ for the neutron with the mass m during the collision of nuclei was determined by eq. (1) with the operator of spin-orbit interaction $\hat{V}_{LS}$

$$(1) \qquad i\hbar\frac{\partial}{\partial t}\Psi(\vec{r},t) = \left\{-\frac{\hbar^2}{2m}\Delta + W(\vec{r},\vec{r}_1(t),\vec{r}_2(t)) + \hat{V}_{LS}(\vec{r},\vec{r}_1(t),\vec{r}_2(t))\right\}\Psi(\vec{r},t).$$

We assume that before contact of the surfaces of spherical nuclei, $W = V_1(|\vec{r} - \vec{r}_1(t)|) + V_2(|\vec{r} - \vec{r}_2(t)|)$, $\hat{V}_{LS} = \hat{V}_{LS,1}(\vec{r} - \vec{r}_1(t)) + \hat{V}_{LS,2}(\vec{r} - \vec{r}_2(t))$.

The initial conditions for the wave functions were obtained using the shell model calculations with the parameters providing neutron separation energies close to the experimental values. The mean field $V_1(r)$, $V_2(r)$ of the Woods-Saxon volume type was used for ^{9}Li, ^{28}Si, and ^{197}Au nuclei. For the ^{6}He nucleus (represented as a system $\alpha + n + n$), a new parametrization of the mean field for external neutrons was used [3, 4] based on the results obtained by Feynman's continual integrals method [5, 6].

2. – Results for ^{6}He+^{197}Au collision

An example of the evolution of the probability density for the external neutrons of the ^{6}He nucleus in the collision with the ^{197}Au nucleus at near-barrier energy was given in ref. [2]. During a slow (adiabatic) relative motion of the colliding nuclei the external neutrons of the ^{6}He nucleus are penetrating into the ^{197}Au nucleus and populating the slowly changing two-centre states, the probability density for which fills a large part of the volume of the target nucleus. The neutron transfer probability $p\,(b, E)$ depending on the impact parameter b and energy E was calculated by integration of the neutron probability density after collision [1-4]. The neutron transfer cross section was calculated by integration of the neutron transfer probability over the impact parameters $b > b_{\min}$

$$\sigma\,(E) = \int_{b_{\min}}^{\infty} p\,(b, E)\, b db, \tag{2}$$

because collisions with $0 \leq b \leq b_{\min}$ lead to fusion.

In the analysis of experimental cross sections for formation of isotopes one must also take into account the possibility of their formation via fusion of colliding nuclei with the subsequent evaporation of nucleons and α-particles. For this purpose, we used the computational code of the statistical model available in the NRV web knowledge base [7].

Comparison of experimental data on the formation of isotopes ^{196}Au and ^{198}Au in the reaction ^{6}He + ^{197}Au with the theoretical calculations is shown in fig. 1. It can be seen that in this case the contribution of fusion-evaporation to the experimental data is negligible due to the high Coulomb barrier of the formed compound nucleus preventing evaporation of α-particles. The formation of ^{198}Au is due to neutron stripping from ^{6}He to the bound states of the Au nucleus. The formation of ^{196}Au is due to neutron pickup from ^{197}Au to the metastable states of the ^{7}He nucleus and neutron knockout by the α-cluster of ^{6}He.

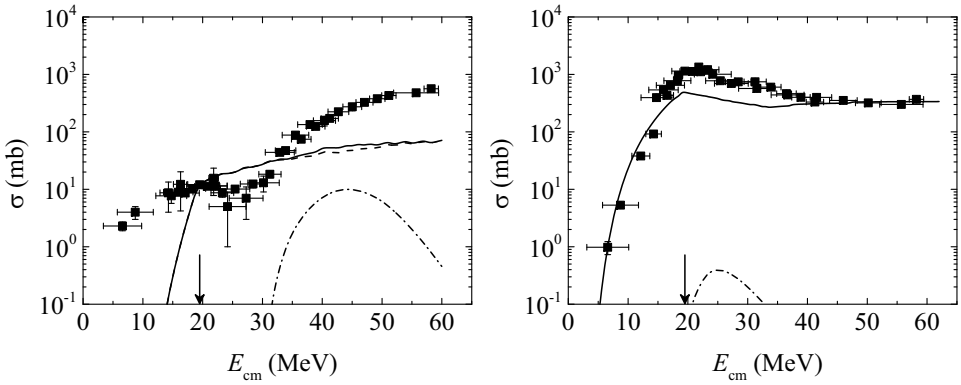

Fig. 1. – The cross sections for formation of isotopes ^{196}Au (left) and ^{198}Au (right) in reaction ^{6}He + ^{197}Au. Symbols are the experimental data from ref. [8]; dash-dotted curves are the results of calculation of fusion-$\alpha 3n$-evaporation (left) and fusion-αn-evaporation (right) within the NRV web knowledge base [7]; dashed curves are the results of neutron transfer (or knockout) calculations within the TDSE approach; solid curves are the sums of the corresponding transfer and fusion-evaporation channels. Arrows indicate the position of the Coulomb barrier.

3. – Results for ^{9}Li + ^{28}Si and ^{6}He + ^{28}Si collisions

Examples of the evolution of the probability density for the external neutrons of the ^{9}Li nucleus in the collision with the ^{28}Si nucleus at different energies were given in ref. [9]. During rapid (diabatic) relative motion, the neutron probability density does not have enough time to fill all the target nucleus, and its change is more local than in the adiabatic case. After the separation of the nuclei, the wave packet in the surface region of the target nucleus remains spreading and rotating with a large angular momentum. At intermediate velocities, a transition from the adiabatic regime to the diabatic one takes place. In the transition regime, rearrangement of outer-skin neutrons of ^{9}Li and halo neutrons of ^{6}He leads to the increase in the neutron probability density between the nuclear surfaces. For ^{7}Li and ^{4}He, this effect is small, therefore, for description of ^{7}Li + ^{28}Si and ^{4}He + ^{28}Si collisions, we use the "frozen" optical potential $\bar{V}(R)$ in the Woods-Saxon form. The parameters were obtained by fitting elastic scattering angular distributions in ref. [9].

For ^{9}Li and ^{6}He nuclei, the real part of the optical potential $\bar{V}(R)$ for nuclei with "frozen" neutrons was supplemented with the diabatic correction arising from an increase in the neutron probability density between the surfaces of the nuclei as they approach,

$$V_{\mathrm{d}}(R, E_{\mathrm{lab}}) = \bar{V}(R) + \eta(E_{\mathrm{lab}})\delta V_{\mathrm{d}}(R, E_{\mathrm{lab}}), \tag{3}$$

$$\delta V_{\mathrm{d}}\left(R(t), E_{\mathrm{lab}}\right) = \int\limits_{\Omega} d^3 r \delta\rho_1(r,t) U_{\mathrm{T}}\left(|\vec{r} - \vec{r}_2(t)|\right), \tag{4}$$

$$\eta(E_{\mathrm{lab}}) = \left\{1 + \exp\left[\frac{1}{\alpha}\left(\langle\varepsilon\rangle - \frac{E_{\mathrm{lab}}}{A}\right)\right]\right\}^{-1}, \tag{5}$$

where U_{T} is the mean field for neutrons in the target nucleus, $\delta\rho_1(r,t) = \rho_1(r,t) - \rho_1^{(0)}(r)$, $\rho_1(r,t)$ is the probability density for the external neutrons of the projectile nucleus, $\rho_1^{(0)}(r)$ is the same density calculated in the absence of interaction of these neutrons with the target nucleus, Ω is the region between the surfaces of the nuclei, A is the mass number of the projectile. The variable parameter $\langle\varepsilon\rangle \approx 10$ MeV determines the position $\bar{E}_{\mathrm{lab}} = \langle\varepsilon\rangle A$ of the transition region, $\alpha \approx 2$ MeV determines its width. The diabatic correction $\delta V_{\mathrm{d}}\left(R, E_{\mathrm{lab}}\right)$ reduces the height $B\left(E_{\mathrm{lab}}\right)$ and shifts to the right the position $R_B\left(E_{\mathrm{lab}}\right)$ of the Coulomb barrier

$$R_B(E_{\mathrm{lab}}) = R_{B,0} + \delta R_B(E_{\mathrm{lab}}). \tag{6}$$

For the imaginary part of the potential we used the approximation with the exponential dependence

$$W(r) = \begin{cases} -W_1, r < R_b \\ -W_1 \exp\left(-\frac{r-R_b}{b}\right), r \geq R_b \end{cases} \tag{7}$$

and the radius R_b increasing according to the shift of the barrier position

$$R_b(E_{\mathrm{lab}}) = R_a + k\delta R_B(E_{\mathrm{lab}}), \tag{8}$$

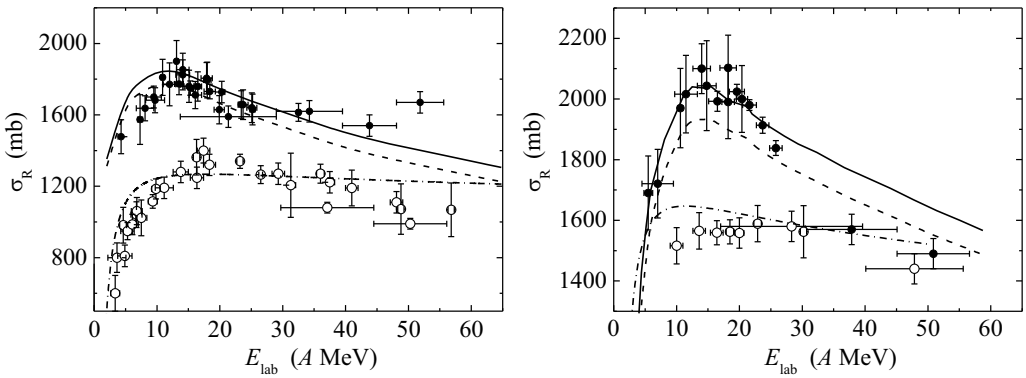

Fig. 2. – The total cross sections for reactions ^{4,6}He + ^{28}Si (left) and ^{7,9}Li + ^{28}Si (right), symbols are the experimental data from [9] and refs. therein: ^{6}He + ^{28}Si and ^{9}Li + ^{28}Si (filled circles), ^{4}He + ^{28}Si and ^{7}Li + ^{28}Si (empty circles); curves are the results of calculation within the TDSE approach combined with the optical model: (left) for $R_a = 5.0$ fm (solid line) and $R_a = 4.8$ fm (dashed line), (right) for $R_a = 5.8$ fm (solid line) and $R_a = 5.6$ fm (dashed line); dash-dotted lines are the results of calculations for the reactions ^{4}He + ^{28}Si (left) and ^{7}Li + ^{28}Si (right).

where $b = 1$ fm, $k = 2$, $R_a = 5.8$ fm for the reaction ^{9}Li + ^{28}Si.

The results of calculation of the total cross sections for reactions ^{4,6}He + ^{28}Si, ^{6,7}Li + ^{28}Si are shown in fig. 2. It can be seen that they are in good agreement with the experimental data from [9] and refs. therein.

4. – Conclusions

The enhancements of the total cross sections for reactions ^{6}He + ^{28}Si and ^{9}Li + ^{28}Si as compared with ^{4}He + ^{28}Si and ^{7}Li + ^{28}Si were explained by the influence of external neutrons of weakly bound projectile nuclei. The time-dependent model shows that the rearrangement of external weakly bound neutrons of nuclei ^{6}He and ^{9}Li during the collision determines the energy dependence of the real and the imaginary parts of the optical potential.

* * *

This work was supported by the Russian Science Foundation (RSF), grant No. 17-12-01170.

REFERENCES

[1] Samarin V. V., *Phys. Atom. Nucl.*, **78** (2015) 128.
[2] Samarin V. V., *EPJ Web Conf.*, **86** (2015) 00040.
[3] Samarin V. V. *et al.*, *J. Phys.: Conf. Ser.*, **724** (2016) 012043.
[4] Naumenko M. A. *et al.*, *Bull. Russ. Acad. Sci.: Phys.*, **81** (2017) 710.
[5] Samarin V. V. and Naumenko M. A., *Bull. Russ. Acad. Sci.: Phys.*, **80** (2016) 283.
[6] Samarin V. V. and Naumenko M. A., *Phys. Atom. Nucl.*, **80** (2017) 877.
[7] Zagrebaev V. I. *et al.*, NRV Web Knowledge Base on Low-Energy Nuclear Physics, `http://nrv.jinr.ru/`.
[8] Penionzhkevich Yu. E. *et al.*, *Eur. Phys. J. A*, **31** (2007) 185.
[9] Penionzhkevich Yu. E. *et al.*, *Phys. Atom. Nucl.*, **80** (2017) 928.